2021 43rd Annual International Conference of the
IEEE Engineering in Medicine & Biology Society (EMBC)
Oct 31 - Nov 4, 2021. Virtual Conference

A Robust and Adaptive Control Algorithm for Closed-Loop Brain Stimulation

Hao Fang[1], *Student Member*, *IEEE*, and Yuxiao Yang[1,2], *Member*, *IEEE*

***Abstract*— Developing closed-loop brain stimulation systems can benefit the treatment of neurological and neuropsychiatric disorders and facilitate brain functions. Current designs of closed-loop controllers have used time-invariant linear models of brain activity to devise non-adaptive controllers. However, unmodeled nonlinear dynamics can happen during real-time closed-loop control, leading to nonlinear uncertainty in the brain activity model. Current non-adaptive controllers cannot track the nonlinear model uncertainty and are not robust to noise, both of which can compromise their control performance. Here, within an $\mathcal{L}_1$ adaptive control framework, we develop a new discrete-time robust and adaptive closed-loop control algorithm that addresses a general form of nonlinear model uncertainty. We conduct Monte Carlo simulations to validate the robust and adaptive control algorithm and show that it significantly outperforms existing closed-loop control algorithms. Our results can facilitate future designs of precise and safe closed-loop brain stimulation systems to treat neurological and neuropsychiatric disorders and modulate brain functions.**

I. INTRODUCTION

Closed-loop control of brain states using brain stimulation such as deep brain stimulation (DBS) [1] is an emerging field in neural engineering because of its potential to treat neurological and neuropsychiatric disorders such as major depressive disorder [2] and to facilitate brain functions such as memory [3]. Different from open-loop stimulation that delivers stimulation without guidance from ongoing brain activity, closed-loop stimulation aims to adjust the stimulation in real-time for precise control of brain states, via using the ongoing brain activity as feedback [2]. Prototype closed-loop stimulation that uses an on-off control law has been used for treating Parkinson's disease [1]. Model-based closed-loop controllers have been proposed for more precise control of brain states [4], [5] and hold promise for providing new therapies for neuropsychiatric disorders [2].

Current designs of model-based closed-loop controllers have largely assumed time-invariant linear models for brain activity [4], [5]. Under this assumption, prior to real-time control, off-line model fitting is performed to fit the model parameters [4], [5], [6]. The fitted parameters are then fixed and used to design a time-invariant closed-loop controller. However, additional nonlinear dynamics can happen during real-time control, for example, due to stimulation-induced neural plasticity [7]. These nonlinear dynamics during real-time control cannot be modeled prior to control. Therefore, the nonlinear dynamics can be represented by a nonlinear uncertainty in the brain activity model. The nonlinear model uncertainty can compromise the control performance of time-invariant controllers [8], creating a major obstacle for achieving precise and safe control of brain states. Therefore, a new closed-loop control algorithm is needed to address nonlinear model uncertainty.

To this end, two major challenges need to be resolved. The first challenge is to design an adaptive controller that can estimate and track the nonlinear model uncertainty during real-time closed-loop control. Current time-invariant controllers are non-adaptive—they do not adapt their parameters over time—, thus cannot track the nonlinear model uncertainty. The second challenge is to design the adaptive controller to be additionally robust to noise. Adaptive controllers are in general sensitive to noise and can be unstable [8], which is unsafe for practical brain stimulation applications. Robust control designs are needed to address noise sensitivity and improve stability. $\mathcal{L}_1$ adaptive control is a powerful control-theoretic method for developing robust and adaptive controllers [8]. However, current discrete-time $\mathcal{L}_1$ adaptive control methods have only assumed a specific linear form of model uncertainty [9], [10], which may not be sufficiently robust to more general forms of nonlinear model uncertainty.

In this work we address the above two challenges by developing a robust and adaptive closed-loop control algorithm within a discrete-time $\mathcal{L}_1$ adaptive control framework. Our first contribution is to design an adaptive algorithm to estimate and track a general form of nonlinear model uncertainty. The controller then, in a closed-loop manner, uses the adaptive estimates to cancel the effect of nonlinear model uncertainty. However, cancellation of model uncertainty should happen only within the bandwidth of the closed-loop system since trying to cancel high-frequency noise increases the controller's sensitivity to noise and can lead to instability [8]. Thus, our second contribution is to add a low-pass filter to the adaptive controller to reduce sensitivity to high-frequency noise for improving robustness. Combining the above two components, we develop a robust adaptive controller for modulating brain states. We next conduct comprehensive Monte Carlo simulations to validate the robust adaptive controller. We show that prior non-adaptive controllers can be unstable under nonlinear model uncertainty and have large control errors. In contrast, the developed robust adaptive controller is stable and significantly reduces the control error by more than 80%. Our results have implications for developing precise and safe closed-loop brain stimulation systems to treat neurological and neuropsychiatric disorders and modulate brain functions.

[1]Department of Electrical and Computer Engineering, University of Central Florida, Orlando, FL, 32816, USA. [2]Disability, Aging, and Technology Faculty Cluster, University of Central Florida, Orlando, FL, 32816, USA (E-mail: yuxiao.yang at ucf.edu)

II. METHODS

A. Dynamic Brain Model with Nonlinear Model Uncertainty

To enable the design of a robust and adaptive closed-loop controller of brain states, we build a discrete-time dynamic state-space model of brain network activity that includes nonlinear uncertain dynamics

$$\begin{cases} x_{t+1} &= Ax_t + Bu_t + f(x_t, u_t) + w_t \\ y_t &= Cx_t + v_t \\ s_t &= Tx_t \end{cases} \tag{1}$$

Here, t is the discrete-time step. $x_t \in \mathbb{R}^{n_x}$ represents a low-dimensional hidden brain state [4]. $y_t \in \mathbb{R}^{n_y}$ represents high-dimensional brain network activity, e.g., multi-channel electrocorticogram (ECoG) or local field potential (LFP) activity [11]. $u_t \in \mathbb{R}$ is the input brain stimulation, such as the amplitude of a DBS pulse train [4]. $s_t \in \mathbb{R}$ represents a neural biomarker that is indicative of behaviors such as mood in depression [12]. s_t is assumed to be a linear function of the hidden brain state [4], [12]. w_t and v_t are white Gaussian noises with zero mean and a joint covariance matrix Q.

The model parameters in (1) are the system matrices $A \in \mathbb{R}^{n_x \times n_x}$, $B \in \mathbb{R}^{n_x \times 1}$, $C \in \mathbb{R}^{n_y \times n_x}$, $T \in \mathbb{R}^{1 \times n_x}$, and the noise covariance matrix $Q \in \mathbb{R}^{(n_x+n_y)\times(n_x+n_y)}$. Based on our prior work [4], [6], [12], we assume that the model parameters can be estimated off-line via data-driven model fitting, thus are known in the controller design.

The critical difference between the dynamic brain model in (1) and our prior work [4], [6], [12] is the additional term $f(x_t, u_t)$. We use a general bounded nonlinear function $f(x_t, u_t) : \mathbb{R}^{n_x} \times \mathbb{R} \to \mathbb{R}^{n_x}$ of both the brain state x_t and the input u_t to model the uncertain dynamics during real-time control, e.g., stimulation-induced neural plasticity [7]. We assume $f(x_t, u_t)$ is unknown since it is real-time model uncertainty and cannot be estimated in off-line model fitting.

Our goal is to design a closed-loop controller to regulate the brain state x_t to track a reference state x_t^{ref} with desired dynamics

$$x_{t+1}^{\text{ref}} = A_m x_t^{\text{ref}} + B^{\text{ref}} s_t^*, \tag{2}$$

such that the controlled neural biomarker s_t tracks a predefined target trajectory s_t^*. Here, $B^{\text{ref}} = BK_g$, $K_g = 1/(T(\mathbb{I} - A_m)^{-1}B)$ ($\mathbb{I}$ is an identity matrix) such that when $s_t^* = s^*$ is a constant, the reference neural biomarker $s_t^{\text{ref}} = Tx_t^{\text{ref}} = s^*$ at steady-state. $A_m \in \mathbb{R}^{n_x \times n_x}$ is picked by the designer to achieve specific transition behavior and stability margin [8].

B. Main Contributions

We aim to design a robust and adaptive controller that can deal with the unknown nonlinear model uncertainty $f(x_t, u_t)$ in (1). Our prior work [4] has only assumed $f(x_t, u_t) = \mathbf{0}$ and designed a non-adaptive controller

$$u_t^{\text{nonad}} = K_x x_t + K_g s_t^*, \tag{3}$$

where K_x is designed to satisfy $A + BK_x = A_m$. Our first contribution is the design of an adaptive controller that can estimate $f(x_t, u_t)$ in real time. Specifically, we augment the non-adaptive component u_t^{nonad} with an adaptive term u_t^{ad}

$$u_t = u_t^{\text{nonad}} + u_t^{\text{ad}}, \quad u_t^{\text{ad}} = -\hat{f}(x_t, u_t), \tag{4}$$

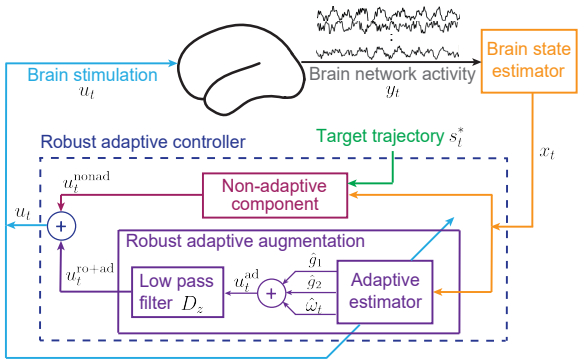

Fig. 1. Robust and adaptive closed-loop control of brain states. The robust adaptive controller (dashed dark blue box) consists of a non-adaptive component (magenta box) and a robust adaptive augmentation (purple box).

where $\hat{f}(x_t, u_t)$ is an adaptive estimate of $f(x_t, u_t)$ (Fig. 1). The adaptive augmentation u_t^{ad} aims to cancel the effect of $f(x_t, u_t)$ on the dynamics of the brain state x_t.

Our second contribution is to improve the robustness of the adaptive augmentation u_t^{ad} to the noise in the adaptive estimate $\hat{f}(x_t, u_t)$. Prior control-theoretic work has used a simple linear term $B(\sigma + \theta x_t)$ in the adaptation to approximate $f(x_t, u_t)$ [9], [10], which has two limitations. It does not model any uncertainty introduced by the input u_t and is exclusively in the range space of the input matrix B. Thus, it is not robust under a general nonlinear uncertainty $f(x_t, u_t)$. In contrast, we use a general approximation $\hat{f}(x_t, u_t)$ that does not have the above limitations. We use the $\mathcal{L}_1$ control theory [8] to further improve the adaptive augmentation u_t^{ad} to be a robust adaptive augmentation

$$u_t^{\text{ro+ad}} = D_t \circledast u_t^{\text{ad}}, \tag{5}$$

where D_t is the impulse response of a low-pass filter and $\circledast$ represents discrete-time convolution (Fig. 1). The low-pass filter facilitates robustness with the motivation that any cancellation of model uncertainty should only happen within the bandwidth of the closed-loop system since aggressive cancellation outside the bandwidth is essentially trying to cancel irreducible noise, and can lead to instability [8].

To summarize, our final robust adaptive controller takes the following form (Fig. 1)

$$u_t = u_t^{\text{nonad}} + u_t^{\text{ro+ad}} = K_x x_t + K_g s_t^* + u_t^{\text{ro+ad}}. \tag{6}$$

Next, we briefly introduce how we compute $u_t^{\text{ro+ad}}$. It is done via two steps; design an adaptive estimator $\hat{f}(x_t, u_t)$ to track nonlinear model uncertainty (section II-C) and design a low-pass filter D_t for achieving robustness (section II-D).

C. Adaptive Estimator

We reformulate the state equation in (1) so that it is amenable for the $\mathcal{L}_1$ adaptive control design. First, we assume that it takes the form $f(x_t, u_t) = \tilde{f}(x_t) + B\Delta\omega u_t$, where $\tilde{f} : \mathbb{R}^{n_x} \to \mathbb{R}^{n_x}$ is an unknown bounded nonlinear function representing uncertainty in the brain state x_t and $\Delta\omega \in \mathbb{R}$ is an unknown bounded constant representing uncertainty of the input gain. Plugging this form of $f(x_t, u_t)$ and control law (6) into the state equation in (1), we have

$$x_{t+1} = A_m x_t + B^{\text{ref}} s_t^* + B\omega u_t^{\text{ro+ad}} + g(x_t),$$

with $\omega = 1 + \Delta\omega$ representing the uncertain input gain and $g(x_t) = \tilde{f}(x_t) + B\Delta\omega K_g s_t^* + B\Delta\omega K_x x_t + w_t$ summarizing other uncertainties. Importantly, we see that $u_t^{\text{ro+ad}}$ can only try to cancel the uncertainty $g(x_t)$ via the range space of B. To facilitate the cancellation of uncertainty, we decompose $g(x_t)$ into two parts $g(x_t) = Bg_1(x_t) + B_{um}g_2(x_t)$, where the first part $Bg_1(x_t)$ is in the range space of B, and the second part $B_{um}g_2(x_t)$ is in the null space of B, i.e., $B_{um} \in R^{n_x \times (n_x - 1)}$ satisfies $B^{'} B_{um} = \mathbf{0}$ and $\text{rank}([B, B_{um}]) = n_x$. We thus rewrite the state equation as

$$x_{t+1} = A_m x_t + B^{\text{ref}} s_t^* + B(\omega u_t^{\text{ro+ad}} + g_1(x_t)) + B_{um} g_2(x_t). \tag{7}$$

With this formulation, we next derive the adaptive estimator for tracking the model uncertainties ω, $g_1(x_t)$ and $g_2(x_t)$. Motivated by prior work [8], to reparametrize (7) for deriving the adaptive estimator, we use the following approximation $g_1(x_t) \approx \sigma_{1,t} + \theta_{1,t} \|x_t\|_\infty$, $g_2(x_t) \approx \sigma_{2,t} + \theta_{2,t} \|x_t\|_\infty$, where $\|x_t\|_\infty = \max_{i=1,\cdots,n_x}(\sup_{0 \le \tau \le t} |x_\tau^i|)$ is the truncated $\mathcal{L}_\infty$ norm [8]. We can then write (7) as

$$\begin{aligned} x_{t+1} = A_m x_t + B^{\text{ref}} s_t^* \quad &+ \quad B(\omega_t u_t + \sigma_{1,t} + \theta_{1,t} \|x_t\|_\infty) \\ &+ \quad B_{um}(\sigma_{2,t} + \theta_{2,t} \|x_t\|_\infty), \end{aligned}$$

which can further be written as

$$x_{t+1} = A_m x_t + B^{\text{ref}} s_t^* + [B, B_{um}] \zeta_t^{'} \phi_t, \tag{8}$$

where $\zeta_t = [\zeta_{1,t}, \zeta_{2,t}]$, $\zeta_{1,t} = [\omega_t, \sigma_{1,t}, \theta_{1,t}]^{'}$, $\zeta_{2,t} = [\mathbf{0}, \sigma_{2,t}, \theta_{2,t}]^{'}$ and $\phi_t = [u_t, 1, \|x_t\|_\infty]^{'}$ ($^{'}$ is transpose). ζ_t contains all the adaptive parameters that need to be estimated.

From (8), we use the standard recursive least-squares method to compute the estimate of ζ_{t+1}, denoted $\hat{\zeta}_{t+1}$, as

$$\hat{\zeta}_{t+1} = \text{Pro}\left(\hat{\zeta}_t + \gamma \phi_t \frac{L(x_{t+1} - A_m x_t - B^{\text{ref}} s_t^*) - \hat{\zeta}_t^{'} \phi_t}{\phi_t^{'} \phi_t}\right), \tag{9}$$

where $L = [B, B_{um}]^{-1}$, $0 < \gamma \le 1$ is the adaptation rate, and $\text{Pro}(\cdot)$ is the standard projection operator to bound the parameters inside their known convex set [8].

Note that in the adaptive estimator (9), we assume that the brain state x_t can be directly observed. In practice, the brain state x_t is often hidden and needs to be estimated from the brain network activity y_t (section II-E).

With the adaptive estimate in (9), the adaptive augmentation in (4) can be computed as

$$u_t^{\text{ad}} = -\hat{\zeta}_{1,t}^{'} \phi_t - H_t \circledast (\hat{\zeta}_{2,t}^{'} \phi_t), \tag{10}$$

where H_t is the impulse response of a specific filter. Here, $\hat{\zeta}_{1,t}^{'} \phi_t$ is used to cancel $g_1(x_t)$. Since u_t^{ad} can only influence the brain state within the range space of B, it cannot completely cancel the term $B_{um}g_2(x_t)$ that is in the null space of B. However, partial cancellation of $B_{um}g_2(x_t)$ at steady state is possible, and it's done via the filter H_t in (10), whose transfer function is $H_z = (T(z\mathbb{I} - A_m)^{-1} B_{um})/(T(z\mathbb{I} - A_m)^{-1} B)$, where H_z is the z-transform of H_t.

D. Robust Controller

With the state equation formulation (7), we derive the low-pass filter in the robust adaptive controller (5) using the $\mathcal{L}_1$ adaptive control theory. We select the transfer function of the low-pass filter D_t—denoted as D_z—to be stable, strictly proper and such that the bandwidth of D_z is sufficiently wider than the closed-loop transfer function, or equivalently the $\mathcal{L}_1$ norm condition $\|P_z(1 - D_z)\|_1 \ll 1$ is satisfied. Here, we use the transfer function of the reference model (2) $P_z = (z\mathbb{I} - A_m)^{-1} B$ to approximate the closed-loop transfer function. With this condition, the low-pass filter D_z preserves the bandwidth of the closed-loop system and only cancels model uncertainty within this bandwidth, thus reduces sensitivity to high-frequency noise and achieves robustness [8]. From (5) and (10), the robust adaptive augmentation is computed as

$$u_t^{\text{ro+ad}} = D_t \circledast (-\hat{\zeta}_{1,t}^{'} \phi_t - H_t \circledast (\hat{\zeta}_{2,t}^{'} \phi_t)). \tag{11}$$

To summarize, equations (9), (11) and (6) give the final robust adaptive controller.

E. Brain State Estimator

To estimate the hidden brain state x_t from the observed brain network activity y_t, we additionally need to use a brain state estimator [4]. Prior work has suggested that for many brain functions and dysfunctions, the hidden brain state often has a much lower dimension than the observed brain activity [13], i.e., $n_x \ll n_y$. Therefore, here, we use a simple estimation $x_t \approx C^\dagger y_t$, where $C^\dagger$ is the Moore–Penrose pseudo-inverse. Using the certainty equivalence principle, we use the state estimate $C^\dagger y_t$ to replace x_t in the adaptation (9).

F. Simulations

We run comprehensive Monte Carlo simulations to test the robust adaptive controller. We simulated ground-truth dynamic brain models using (1), where we use a fully-connected feed-forward deep neural network (5 layers with 10 neurons at each layer) to simulate the nonlinear model uncertainty $f(x_t, u_t)$. We in total simulated 9000 ground-truth dynamic brain models with the dimension of the hidden brain state n_x ranging from 2 to 10. We fixed the dimension of the brain network activity $n_y = 3 \times n_x$ for each model. In each model, the system matrices and the noise covariance matrix are randomly generated in the same way as our prior work [4], and the weight matrices in the deep neural network are generated as standard random Gaussian matrices. In general, the simulated ground-truth dynamic brain model can be unstable. The target trajectory is set as a constant value of $s^* = 10$ in all simulations.

We compare the robust adaptive controller with three other controllers: the non-adaptive controller in our prior work [4] (see (3)); the adaptive controller in [10], which is not robust to nonlinear uncertainty (termed non-robust adaptive controller); an ideal controller that theoretically has the best possible control performance. The ideal controller is constructed by replacing the adaptive estimates in (11) with the ground-truth $g_1(x_t)$ and $g_2(x_t)$.

We use the normalized steady-state control error e to quantify the control performance of each controller relative to the target value s^*, $e = \sqrt{\sum_{t=t_0}^{T}(s_t - s^*)^2/(T - t_0)}/s^* \times$

100%, where s_t is the controlled neural biomarker in closed loop, t_0 is the starting time point of steady state and T is the total control time period in simulation.

III. Results and Discussions

For two example dynamic brain models (Fig. 2a), we observed that under nonlinear model uncertainty, the non-adaptive controller did not track the target level and had a large control error ($e = 71\%$). While the non-robust adaptive controller reduced the control error, it still had a larger control error compared with the ideal controller and did not track the target ($e = 33\%$). By contrast, the robust adaptive controller tracked the target and significantly reduced the control error ($e = 11\%$), performing similarly with the ideal controller ($e = 10\%$). Note that the control error of the ideal controller was not zero because the ground-truth dynamic brain models had noise.

Monte Carlo simulation results confirmed the above observations. First, for more than 50% of the ground-truth brain dynamic models, the non-adaptive controller and the non-robust adaptive controller resulted in unstable control. Therefore, under general nonlinear model uncertainty, the two controllers could have severe instability issues and would be unsafe in practical applications of controlling brain states. In contrast, in all the ground-truth brain dynamic models, the robust adaptive controller was stable. The result suggested the stability of the robust adaptive controller under general nonlinear model uncertainty. Providing theoretical stability analysis for the robust adaptive controller is an important future direction to ensure safety in practical applications.

Second, consistent with the two examples, compared with the non-adaptive controller, the robust adaptive controller had a significantly smaller control error ($23.73\% \pm 0.56\%$ v.s. $132.9\% \pm 1.37\%$, mean $\pm$ s.e.m., Wilcoxon signed-rank test $P < 10^{-50}$; Fig. 2b), reducing the non-adaptive control error relatively by 82.1%. Compared with the non-robust adaptive controller, the robust adaptive controller also showed smaller control error ($23.73\% \pm 0.56\%$ v.s. $119.9\% \pm 1.40\%$, Wilcoxon signed-rank test $P < 10^{-50}$; Fig. 2b), reducing the non-robust adaptive control error relatively by 80.2%. Moreover, the robust adaptive controller performed close to the ideal controller ($23.73\% \pm 0.56\%$ v.s. $23.47\% \pm 0.53\%$; Fig. 2b). These results indicates that the developed robust adaptive controller could achieve stable and precise control of brain states under a wide range of nonlinear model uncertainties. One future direction is to validate the generalizability of the controller by simulating more realistic biophysical models, e.g., neuronal spiking models for Parkinson's disease [1]. Another future direction is to combine our control algorithm with the recursive estimator developed in our prior work [14] to achieve better estimation and control of the hidden brain state from the observed brain activity.

IV. Conclusions

In this work, we develop a new discrete-time robust and adaptive algorithm for closed-loop control of brain states. Our closed-loop control algorithm uses an adaptive estimator

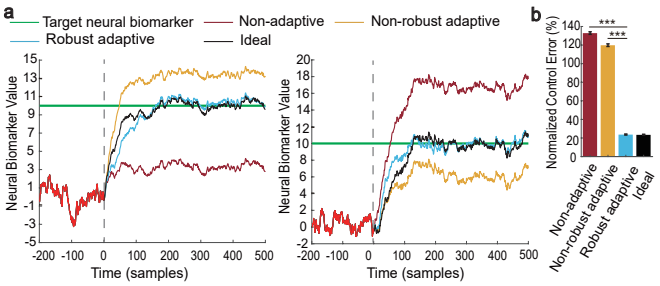

Fig. 2. (a) Two example closed-loop simulations. Dashed line represents the starting point of applying control. (b) Control errors of different controllers (Bar represents mean, whiskers represents s.e.m., $***, P < 0.0005$).

to track a general form of nonlinear model uncertainty and uses a low-pass filter to reduce sensitivity to high-frequency noise for achieving robustness. Monte Carlo simulation results show that the developed algorithm is stable and outperforms existing controllers. Our results have implications for future designs of intelligent and safe neuromodulation systems for treating neurological and neuropsychiatric disorders and modulating brain functions.

References

[1] M. Vissani, I. U. Isaias, and A. Mazzoni, "Deep brain stimulation: a review of the open neural engineering challenges," *J. Neural Eng.*, vol. 17, no. 5, p. 051002, 2020.

[2] M. M. Shanechi, "Brain–machine interfaces from motor to mood," *Nat. Neurosci.*, vol. 22, no. 10, pp. 1554–1564, 2019.

[3] Y. Ezzyat, P. A. Wanda, D. F. Levy, A. Kadel, A. Aka, I. Pedisich, M. R. Sperling, A. D. Sharan, B. C. Lega, A. Burks, *et al.*, "Closed-loop stimulation of temporal cortex rescues functional networks and improves memory," *Nat. Commun.*, vol. 9, no. 1, pp. 1–8, 2018.

[4] Y. Yang, A. T. Connolly, and M. M. Shanechi, "A control-theoretic system identification framework and a real-time closed-loop clinical simulation testbed for electrical brain stimulation," *J. Neural Eng.*, vol. 15, no. 6, p. 066007, 2018.

[5] M. F. Bolus, A. A. Willats, C. J. Rozell, and G. B. Stanley, "State-space optimal feedback control of optogenetically driven neural activity," *J. Neural Eng.*, 2020.

[6] Y. Yang, S. Qiao, O. G. Sani, J. I. Sedillo, B. Ferrentino, B. Pesaran, and M. M. Shanechi, "Modelling and prediction of the dynamic responses of large-scale brain networks during direct electrical stimulation," *Nat. Biomed. Eng.*, pp. 1–22, 2021.

[7] P. V. Massey and Z. I. Bashir, "Long-term depression: multiple forms and implications for brain function," *Trends Neurosci.*, vol. 30, no. 4, pp. 176–184, 2007.

[8] N. Hovakimyan and C. Cao, *$\mathcal{L}_1$ adaptive control theory: Guaranteed robustness with fast adaptation*. SIAM, 2010.

[9] H. Jafarnejadsani and N. Hovakimyan, "Optimal filter design for a discrete-time formulation of $\mathcal{L}_1$-adaptive control," in *AIAA Infotech@ Aerospace*, 2015, p. 0119.

[10] M. Elnaggar, M. S. Saad, H. A. Fattah, and A. L. Elshafei, "Discrete time $\mathcal{L}_1$ adaptive control for systems with time-varying parameters and disturbances," in *55th Proc. IEEE Conf. Decis. Control*, 2016, pp. 2115–2120.

[11] B. Pesaran, M. Vinck, G. T. Einevoll, A. Sirota, P. Fries, M. Siegel, W. Truccolo, C. E. Schroeder, and R. Srinivasan, "Investigating large-scale brain dynamics using field potential recordings: analysis and interpretation," *Nat. Neurosci.*, vol. 21, no. 7, pp. 903–919, 2018.

[12] O. G. Sani, Y. Yang, M. B. Lee, H. E. Dawes, E. F. Chang, and M. M. Shanechi, "Mood variations decoded from multi-site intracranial human brain activity," *Nat. Biotechnol.*, vol. 36, no. 0, pp. 954–961, 2018.

[13] J. P. Cunningham and M. Y. Byron, "Dimensionality reduction for large-scale neural recordings," *Nat. Neurosci.*, vol. 17, no. 11, pp. 1500–1509, 2014.

[14] Y. Yang, P. Ahmadipour, and M. M. Shanechi, "Adaptive latent state modeling of brain network dynamics with real-time learning rate optimization," *J. Neural Eng.*, vol. 18, no. 3, p. 036013, 2021.